Method of Moments (MoM) Modeling for Resonating Structures: Propagation inside a Parallel Plate Waveguide

G. Apaydin [1], L. Sevgi [2,3]

[1] Department of Electrical-Electronics Engineering
Zirve University, Gaziantep, 27260, Turkey
gokhan.apaydin@zirve.edu.tr

[2] Department of Electronics and Communications Engineering
Dogus University, Istanbul, 34722, Turkey
lsevgi@dogus.edu.tr

[3] Department of Electrical and Computer Engineering
University of Massachusetts Lowell (UML), Massachusetts, 01854, USA
levent_sevgi@uml.edu

Abstract **─** Method of Moments (MoM) modeling inside resonating structures is discussed and a novel approach called Multi-MoM (Mi-MoM) is proposed. Propagation inside a two-dimensional (2D) non-penetrable parallel plate waveguide is taken into account. The Mi-MoM results are compared with the analytical reference solution. Practical ways of different source representations (untilted/tilted Gaussian beams) are also presented. Finally, surface irregularities inside the waveguide and their effects on the propagation are modeled with both Mi-MoM and the Split-Step Parabolic Equation (SSPE) method.

Index Terms - computational electromagnetics, gaussian beam, Green's function, method of moments, mode summation, MoM, parallel plate waveguide, propagation, split step parabolic equation, SSPE.

I. INTRODUCTION

Method of Moments (MoM) [1] is one of the oldest numerical electromagnetic (EM) model. In this method, first a discrete model of the object under investigation is created from small pieces (compared to wavelength) called segments or patches. Everything on these segments is assumed constant. Then, an NxN system of equations is built with N unknown segment/patch currents, N known segment voltages, calculated from the Green's function of the problem, and known NxN segment/patch impedances. The model is closed-form and stable, but necessitates high memory and high speed computers especially for high frequency applications (it requires N^3 operations). It requires the Green's function of the problem. MoM has been successfully applied to broad range of EM scattering problems (see, for example [1-4] for some of the applications). MoM with some acceleration techniques (e.g., Forward-Backward Spectral Acceleration - FBSA) has also been applied to propagation problems [5-7], especially to long-range ground wave propagation over irregular and lossy Earth.

Propagation modeling inside waveguides with irregular and lossy boundaries has become important because of signaling requirements through railway tunnels, communication in mines, screening in printed circuit boards (PCB), etc. The Split-Step Parabolic Equation (SSPE) and Finite Element based PE models to these guiding structures have been developed and calibrated against analytical reference data in [8]. MoM suffers from resonances in these waveguiding structures [9-10] therefore its direct application is a challenge. Here, a novel Multi-Iteration MoM model (Mi-MoM) is introduced for this purpose. Propagation inside a two-dimensional (2D), non-penetrable parallel plate waveguide is taken into account. The novel Mi-MoM model is compared

Submitted On: July 23, 2012
Accepted On: Sept. 17, 2012

against analytical reference data (generated from the exact mode summation model), as well as against SSPE [8-9].

Propagation inside a parallel plate waveguide is an interesting EM problem where both analytical and numerical models can be tested one against the others [11-12]. It can also be used for calibration. The Green's function solution (i.e., EM response of a line source) is exact but requires infinite number of mode (eigenfunction) summation [11]. This is a numerical challenge especially in the near vicinity of the line source. Modes are grouped into two; propagating modes (with real eigenvalues) and evanescent modes (with complex eigenvalues). The number of propagating modes depends on the frequency and width of the plate. A tilted directional antenna can also be located inside and can be modeled in terms of modes, but modal excitation coefficients become complex. This is another numerical challenge, especially at high frequencies when the number of propagating modes is extremely high. The modes are global therefore do not suffer from local problems, but extraction of modal excitation coefficients is crucial when generating reference solutions. Analytical exact solution can also be constructed in terms of rays which are local wave pieces; again summation of infinite number of rays is required for the line source excitation [12]. Moreover, eigenray extraction might have numerical problems.

II. THE 2D GREEN'S FUNCTION PROBLEM AND ANALYTICAL REFERENCE SOLUTION

The 2D parallel plate waveguide is pictured in Fig. 1. Here, x and z are the transverse and longitudinal coordinates, respectively. The structure is infinite along y-direction ($\partial / \partial y \equiv 0$). The width of the waveguide is a. The PEC boundaries are assumed Dirichlet-type for the $\mathrm{TE_z}$ (transverse electric with respect to z) problem and Neumann-type for the $\mathrm{TM_z}$ (transverse magnetic with respect to z) problem (see [13] for TE/TM discussions).

Since the $\mathrm{TE_z}$ and $\mathrm{TM_z}$ sets are decoupled, each can be excited independently of the other by appropriate selection of the sources, **J** and **M**. The line sources M_x, M_z, J_y excite the $\mathrm{TE_z}$ set, whereas the line sources M_y, J_x, J_z excite the $\mathrm{TM_z}$ set. Further simplification can be obtained by setting the source components M_x=0, M_z=0 for the $\mathrm{TE_z}$ set, and J_x=0, J_z=0 for the $\mathrm{TM_z}$ set.

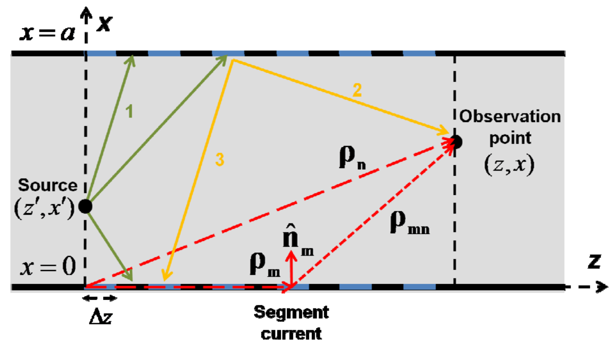

Fig. 1. The non-penetrable (PEC) parallel plate waveguide, x: height, z: range and tilt is measured from z-axis ("+" for upwards, "-" for downwards).

The Green's function problem (under $\exp(j\omega t)$ time dependence) associated with both the $\mathrm{TE_z}$ set (when $M_x=M_z=0$) and the $\mathrm{TM_z}$ set (when $J_x=J_z=0$) is postulated as:

$$\left\{\frac{\partial^2}{\partial x^2}+\frac{\partial^2}{\partial z^2}+k_0^2\right\}g(x,z;x',z')=\delta(x-x')\delta(z-z'),\quad(1)$$

with the boundary conditions (BC)

$$g(x,z;x',z')=0 \quad \text{at } x=0,a \quad (\mathrm{TE_z}),\quad(2a)$$

$$\frac{\partial}{\partial x}g(x,z;x',z')=0 \quad \text{at } x=0,a \quad (\mathrm{TM_z}),\quad(2b)$$

$$g(x,z;x',z')=0 \quad \text{as } z\to\pm\infty\,.\quad(2c)$$

Here, (x',z') and (x,z) specify source and observation points, respectively, $\delta(\cdot)$ is the Dirac delta function, $k_0=2\pi/\lambda=\omega\sqrt{\varepsilon_0\mu_0}$ is the free-space wave-number, and λ is the free-space wavelength.

The Green's function $g(x,z;x',z')$ can be obtained as

$$g(x,z;x',z')=\tilde{g}(z;z')+\frac{2}{a}\sum_{m=1}^{\infty}\frac{e^{-jk_{zm}|z-z'|}}{2jk_{zm}}\Psi(k_{xm}x)\Psi(k_{xm}x'),\quad(3)$$

$$\tilde{g}(z;z')=0,\Psi(x)=\sin(x)\,(\mathrm{TE_z}),\quad(4a)$$

$$\tilde{g}(z;z')=\frac{1}{a}\frac{e^{-jk_0|z-z'|}}{2jk_0},\Psi(x)=\cos(x)\,(\mathrm{TM_z}),\quad(4b)$$

where $k_{xm}=m\pi/a$, $k_{zm}=\sqrt{k_0^2-k_{xm}^2}$. The line-source-excited fields are then given by either

$E_y = j\omega\mu_0 g$ or $H_y = j\omega\varepsilon_0 g$ for the TE$_z$ and TM$_z$ cases, respectively. The remaining field components can be calculated from

$$H_x = \frac{1}{j\omega\mu_0}\left\{\frac{\partial E_y}{\partial z} - M_x\right\}, \tag{5a}$$

$$H_z = -\frac{1}{j\omega\mu_0}\left\{\frac{\partial E_y}{\partial x} + M_z\right\}, \tag{5b}$$

for the TE$_z$ model and

$$E_x = -\frac{1}{j\omega\varepsilon_0}\left\{\frac{\partial H_y}{\partial z} + J_x\right\}, \tag{6a}$$

$$E_z = \frac{1}{j\omega\varepsilon_0}\left\{\frac{\partial H_y}{\partial x} - J_z\right\}, \tag{6b}$$

for the TM$_z$ model.

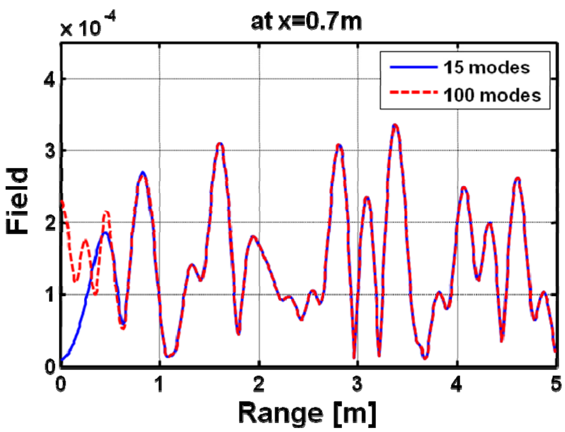

Fig. 2. Field vs. z (TM$_z$ case): (Solid) only 15 propagating modes, (Dashed) The first 100 modes (a=1 m, $z' = 0$, $x' = 0.3$ m, $x = 0.7$ m, $k_0 a = 50$).

A short MatLab code is prepared for the calculation of field distribution inside the parallel plate waveguide in terms of mode summation for both polarizations. An example is shown in Fig. 2. Here, longitudinal variation of the field inside a 1m-wide plate at $x = 0.7$ m is pictured. The line source is at $x' = 0.3$ m. The number of propagating modes for the sets of parameters listed in the figure is 15. The two curves belong to the summation of the first 15 and 100 modes. As observed, at a distance beyond $z = 0.5$ m (i.e., after 3-4 λ distance) only propagating modes contribute. Figure 3 displays field vs. x at two different distances ($z = 2\lambda$ and $z = 20\lambda$). As observed, the contribution of only propagating modes at $z = 2\lambda$ is not enough to build the correct field distribution.

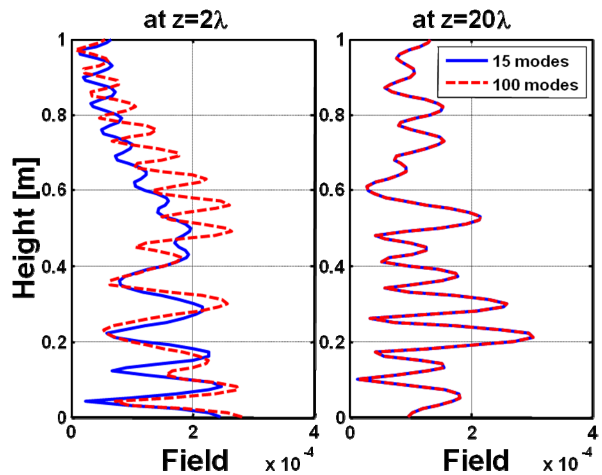

Fig. 3. Field vs. x (TM$_z$ case): (Solid) only 15 propagating modes, (Dashed) The first 100 modes ($a = 1$ m, $z' = 0$, $x' = 0.3$ m, $k_0 a = 50$).

The line source is a theoretical antenna. In practice, a directive antenna is used in many applications. This antenna can be tilted upwards or downwards. A directive antenna with tilt-capability is usually modeled by injecting a vertical field distribution (e.g., a complex Gaussian function) in analytical and numerical simulations. It is therefore a challenge to compare models using line source excitations models with directive antennas; even data normalization may not be a solution in many cases. One solution in modeling a tilted (Gaussian) beam excitation is to use a line source at a specific horizontal position and then determine the ray excitation coefficients according to their departure angles.

The tilted Gaussian source $f(x, z')$ inside a parallel plate waveguide at $z = z'$ may be represented in terms of modal summation as:

$$f(x, z') = \sum_{m=m_0}^{M} c_m(z')\, v_m \Psi(k_{xm} x), \tag{7}$$

where M is the highest mode that should be included for the specified excitation (and depends on the specified accuracy), v_m is the normalization constant calculated from

$$v_m = \left(\int_{x=0}^{a} \Psi^2 (k_{xm} x) dx \right)^{-1/2}, \tag{8}$$

and $c_m(z')$ is the modal excitation coefficient, numerically derived from transverse orthonormality condition:

$$c_m(z') = v_m \int_0^a f(x, z') \, \Psi(k_{xm} x) \, dx \,. \tag{9}$$

The initial field profile $f(x,0)$ at $z' = 0$ is generated from a tilted Gaussian pattern

$$f(x,0) = \exp\left[-jk_0 x \sin\theta_{elv} - \frac{(x - x')^2}{w^2} \right], \tag{10}$$

where $w = \sqrt{2\ln 2} / (k_0 \sin(\theta_{bw}/2))$. The tilted antenna pattern is specified by its transverse position (x'), beamwidth (θ_{bw}) and tilt (elevation) angle (θ_{elv}). Note that, Ψ again shows either Sine or Cosine function starting from either m_0=1 or m_0=0 for the TE_z and TM_z cases, respectively. The number of modes would be finite for numerical computations. It is common to choose a vertically extending Gaussian function with arbitrary location having vertical elevation angle in the range of ±90° (plus for upwards, minus for downwards). Note that the modal excitation coefficient c_m is real for a real source function without any tilt, and becomes complex if the source is tilted.

It should be noted that, reference data can best be generated from analytical exact solution if numerically computed accurately. The mode summation solution is exact but necessitates infinite number of terms with complex excitation coefficients for tilted directive antennas.

Figure 4 illustrates reliability of the reference data for a tilted Gaussian antenna. Here, field vs. x at two different z points for the same set of parameters, but for a directive antenna tilted 30° downwards with 45° beamwidth. The solid line belongs to data generated with the mode summation model. The dashed line belongs to the well-known Split-Step Parabolic Equation (SSPE) model [9]. A perfect agreement indicates the reliability of the reference data under both line source and directive antenna excitations.

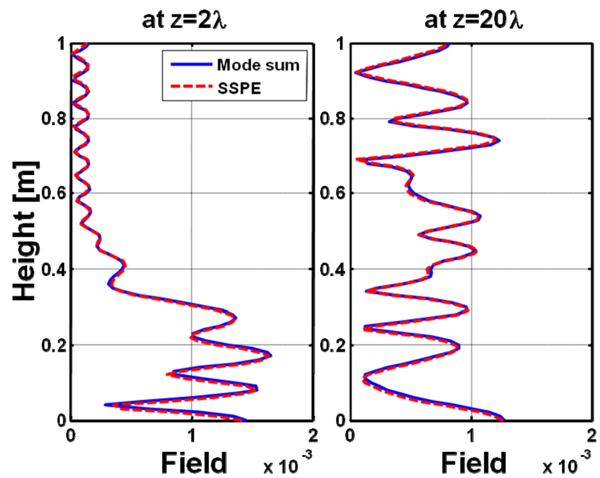

Fig. 4. Field vs. x (TM_z case): (Solid) Mode sum with 49 modes, (Dashed) SSPE ($a = 1$ m, $z' = 0$, $x' = 0.3$ m, $k_0 a = 50$, $dz = dx = 0.01$ m, $\theta_{bw} = 45°$, $\theta_{elv} = -10°$).

III. PARALLEL PLATE WAVEGUIDE AND METHOD OF MOMENT MODELING

Method of Moments (MoM) technique can be used to find propagation of horizontally (TE_z case) and vertically (TM_z case) polarized waves by using the Electric Field Integral Equation (EFIE) and the Magnetic Field Integral Equation (MFIE), respectively. Open region propagation over irregular ground and/or rough surface has been successfully modeled with MoM (see, for example, [5-7] among a huge number of reference list which cannot be included here). In the classical MoM, the integral equation is converted to the corresponding matrix equation via the discretization of the ground/surface. Then, an NxN system of equations $[V] = [Z][I]$ is constructed and is solved numerically. Here, $[I]$ contains the unknown segment currents, $[V]$ contains segment voltages excited by the source, $[Z]$ is the NxN impedance matrix of the ground/surface. Solution of this system yields the unknown segment currents. Superposition of the contributions of the segment currents via the Green's function of the problem yields the ground-scattered field. Finally, the total field is obtained by adding the incident field [6].

The classical MoM approach can be enhanced to model propagation inside waveguiding structures. This is achieved by using the free-space Green's functions with a multi-iterative approach to build in the presence of the multiple reflections due to the conducting walls. Figure 1 shows MoM discretization and related parameters. Ray 1, shown as a sample, induces segment currents because of the external source. Ray 2 contributes to the field because of the induced segment currents. Ray 3 represents higher order effects on bottom segments caused by top segment currents. Necessary formulae for both polarizations are as summarized in [1,2,7]:

$\mathbf{TE_z}$ case

$$V_m = -E_y^{inc}(\boldsymbol{\rho}_\mathbf{m}) = -E_0 \frac{e^{-jk_0 d_m}}{\sqrt{k_0 d_m}}, \quad (11a)$$

$$d_m = \sqrt{[x(\boldsymbol{\rho}_\mathbf{m}) - x']^2 + [z(\boldsymbol{\rho}_\mathbf{m}) - z']^2}, \quad (11b)$$

$$Z_{nm} \cong \begin{cases} -\dfrac{k_0 \eta_0 \Delta z}{4} H_0^{(2)}\left(k_0 |\boldsymbol{\rho}_\mathbf{n} - \boldsymbol{\rho}_\mathbf{m}|\right), m \neq n \\ -\dfrac{k_0 \eta_0 \Delta z}{4}\left[1 - j\dfrac{2}{\pi}\log\left(\dfrac{\gamma k_0 \Delta z}{4e}\right)\right], m = n \end{cases}, \quad (11c)$$

$$E_y^{sc}(\boldsymbol{\rho}_\mathbf{n}) \cong -\frac{k_0 Z_0 \Delta z}{4} \sum_{m=1}^{N} I_m H_0^{(2)}\left(k_0 |\boldsymbol{\rho}_\mathbf{n} - \boldsymbol{\rho}_\mathbf{m}|\right), \quad (11d)$$

$$E_y^{tot} = E_y^{sc} + E_y^{inc}, \quad (11e)$$

TMz case

$$V_m = -H_y^{inc}(\boldsymbol{\rho}_\mathbf{m}) = -\frac{E_0}{\eta_0} \frac{e^{-jk_0 d_m}}{\sqrt{k_0 d_m}}, \quad (12a)$$

$$d_m = \sqrt{[x(\boldsymbol{\rho}_\mathbf{m}) - x']^2 + [z(\boldsymbol{\rho}_\mathbf{m}) - z']^2}, \quad (12b)$$

$$Z_{nm} \cong \begin{cases} j\dfrac{k_0 \Delta z}{4} H_1^{(2)}\left(k_0 |\boldsymbol{\rho}_\mathbf{n} - \boldsymbol{\rho}_\mathbf{m}|\right)(\hat{\mathbf{n}}_\mathbf{m} \cdot \hat{\boldsymbol{\rho}}_\mathbf{nm}), m \neq n \\ 0.5, m = n \end{cases}, \quad (12c)$$

$$H_y^{sc}(\boldsymbol{\rho}_\mathbf{n}) \cong \frac{jk_0 \Delta z}{4} \cdot \sum_{m=1}^{N} I_m H_1^{(2)}\left(k_0 |\boldsymbol{\rho}_\mathbf{n} - \boldsymbol{\rho}_\mathbf{m}|\right)(\hat{\mathbf{n}}_\mathbf{m} \cdot \hat{\boldsymbol{\rho}}_\mathbf{nm}), \quad (12d)$$

$$H_y^{tot} = H_y^{sc} + H_y^{inc}, \quad (12e)$$

where Δz is the segment length, $\eta_0 \approx 120\pi$ is the intrinsic impedance of free space, $H_0^{(2)}$ and $H_1^{(2)}$ are the second kind Hankel functions with order zero and one, respectively, $\gamma \approx 1.781$ is the exponential of the Euler constant, $\hat{\mathbf{n}}_\mathbf{m}$ denotes the unit normal vector of the plate at $\boldsymbol{\rho}_\mathbf{m}$, and $\hat{\boldsymbol{\rho}}_\mathbf{nm}$ is the unit vector in the direction from source $\boldsymbol{\rho}_\mathbf{m}$ to the receiving element $\boldsymbol{\rho}_\mathbf{n}$.

The Mi-MoM procedure may be outlined as follows:

- First, discretize top and bottom boundaries. Use N segments for the lower and N segments for the upper boundaries. Label all segments from 1 to N in a way that Segment 1 and Segment N+1 have the same horizontal (i.e., z) coordinate (i.e., parallel to each other).
- Calculate segment currents $[I]$ from $[I] = [Z]^{-1}[V]$ and scattered/total fields using either E_y^{inc} in (11a) or H_y^{inc} in (12a) for TE_z and TM_z polarizations, respectively.
- For a given source point, calculate distances to all segments and segment voltages, using either E_y^{inc} in (11b) or H_y^{inc} in (12b) for TE_z and TM_z polarizations, respectively. This will yield $[V]$.
- Calculate the impedance matrix Z_{nm} from either (11c) or (12c) for TE_z and TM_z polarizations, respectively.
- The segment currents induced by the external source on the top plate excite field on segments on the bottom plate and a vice versa. For the first segment on the bottom plate, calculate distances to all segments on the top plate and segment voltages, using either E_y^{inc} in (11a) or H_y^{inc} in (12a) for TE_z and TM_z polarizations, respectively. Repeat this for all segments on the bottom plate and find out the voltages on the top plate caused by the segments on the bottom plate.
- Do the same for the segments on the top plate and find out the voltages on the bottom plate caused by the segments on the top plate. This will yield second round $[V]$.
- Use the same impedance matrix Z_{nm} and calculate second round segment currents $[I]$ from $[I] = [Z]^{-1}[V]$ and scattered/total fields using either E_y^{sc} in (11d/11e) or H_y^{sc} in (12d/12e) for TE_z and TM_z cases, respectively.

- Repeat the procedure and find out third round segment currents and scattered/total fields caused by these current.
- Repeat the whole procedure until a desired accuracy is reached.

An alternative way is to find out first round segment currents and then use the Image Method (IM). First, all segment currents of upper and lower plates are obtained. Then, boundaries are removed and image segments are added with respect to the upper and lower plates. Finally, field contributions from the currents of segments and image-segments are superposed at the receiver.

Two examples for the Mi-MoM procedure are given in Figs. 5 and 6. Figure 5 shows propagation factor (PF) (calculated field divided by its free-space value in dB) vs. z at a fixed x inside the parallel plate waveguide calculated with mode summation and Mi-MoM methods. As shown, very good agreement is obtained. As expected, Mi-MoM suffers from end-point effects, since segments before the first one and after the last one are neglected [6]. In order to overcome insufficiency of the MoM end-point effects one needs to extend the horizontally at least one or two wavelengths at both ends.

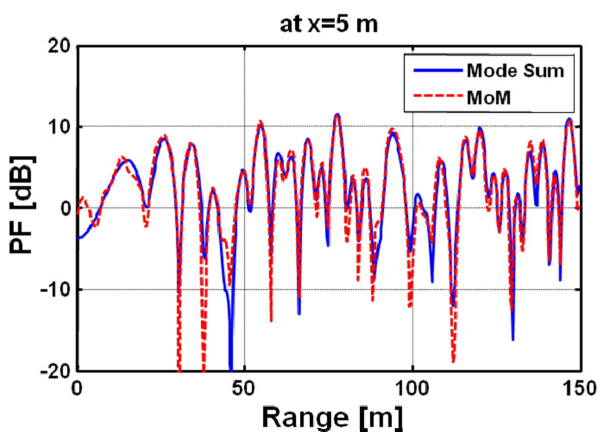

Fig. 5. Propagation factor vs. z (TM_z case): (Solid) Mode sum, (Dashed) Mi-MoM ($a = 100$ m, $z' = 0$, $x' = 50$ m, $x = 5$ m, $k_0 a = 209.5$).

Figure 6 shows field vs. x at two different z points, again calculated with mode summation and Mi-MoM methods. As observed, the agreement is very good. Note that, the agreement in Fig. 5 is better than the agreement in Fig. 6; this is merely because of the frequency used in these examples ($k_0 a = 209.5$ in Fig. 5, but $k_0 a = 50$ in Fig. 6). The accuracy of Mi-MoM solution increases with frequency (i.e., with $k_0 a$).

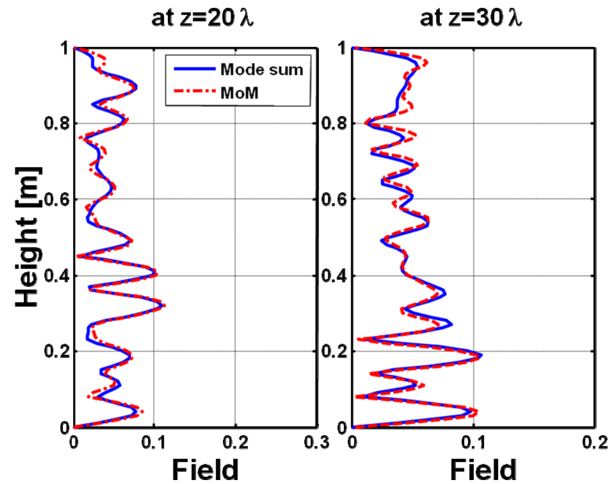

Fig. 6. Field vs. x (TE_z case): (Solid) Mode sum, (Dashed) Mi-MoM, $a = 1$ m, $z' = 0$, $x' = 0.4$ m, $k_0 a = 50$.

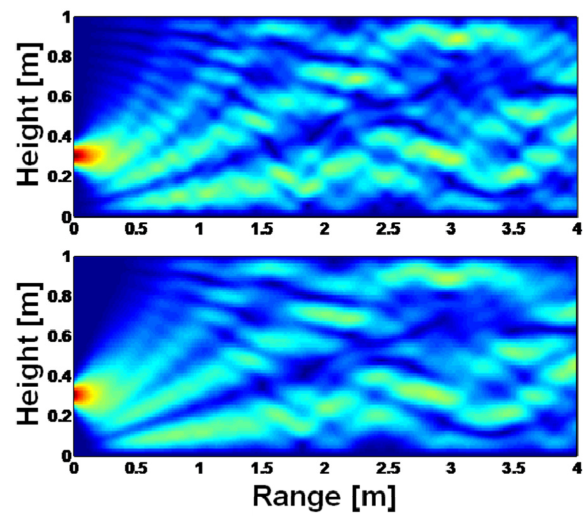

Fig. 7. The field map (TE_z case): (Top) Mode sum with 42 modes, (Bottom) Mi-MoM with 40 iterations, $a = 1$ m, $z' = 0$, $x' = 0.3$ m ($k_0 a = 50$, $dz = dx = 0.01$ m, $\theta_{bw} = 45°$, no tilt).

Figures 7-9 belong to comparisons for directive antennas. As observed, the agreement between Mi-MoM results and the reference data is impressive even for these highly resonating/oscillatory variations.

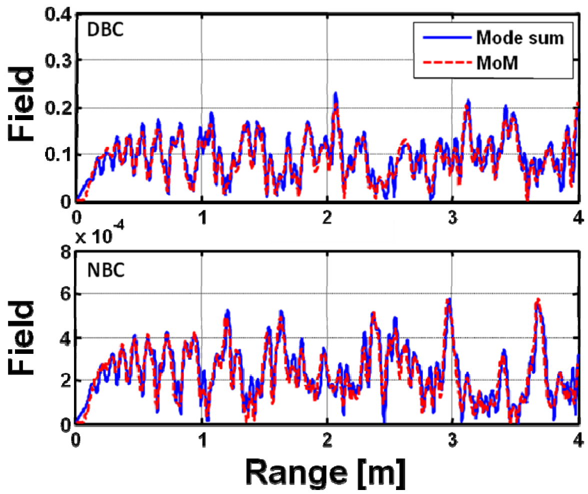

Fig. 8. Field vs. z at $x = 0.2$ m: (Top) TE_z case, (Bottom) TM_z case, (Solid) Mode sum with 282 modes, (Dashed) Mi-MoM with 50 iterations ($a = 1$ m, $z' = 0$, $x' = 0.4$ m, $k_0 a = 200$, $dz = dx = 0.0025$ m, $\theta_{bw} = 80°$, no tilt).

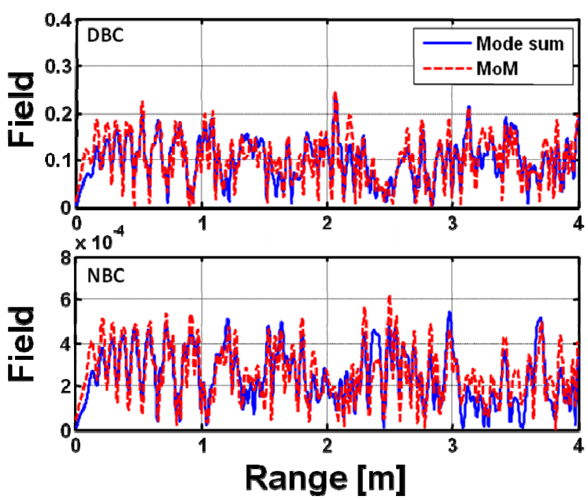

Fig. 9. Field vs. z at $x = 0.2$ m: (Top) TE_z case, (Bottom) TM_z case, (Solid) Mode sum with 298 modes, (Dashed) Mi-MoM with 50 iterations ($a = 1$ m, $z' = 0$, $x' = 0.4$ m, $k_0 a = 200$, $dz = dx = 0.0025$ m, $\theta_{bw} = 45°$, $\theta_{elv} = -20°$).

The final example belongs to a more realistic case. Figure 10 presents Mi-MoM vs. SSPE comparisons inside a PEC parallel plate waveguide with some irregularities on the bottom plate. Figure 10a presents the structure. Here, two Gaussian-shaped hills are shown on the bottom plate. Figure 10b shows 3D field map inside the plate. Figure 10c belongs to the z variations of the field at $x = 0.4$ m for the TE_z polarization computed with Mi-MoM and SSPE methods.

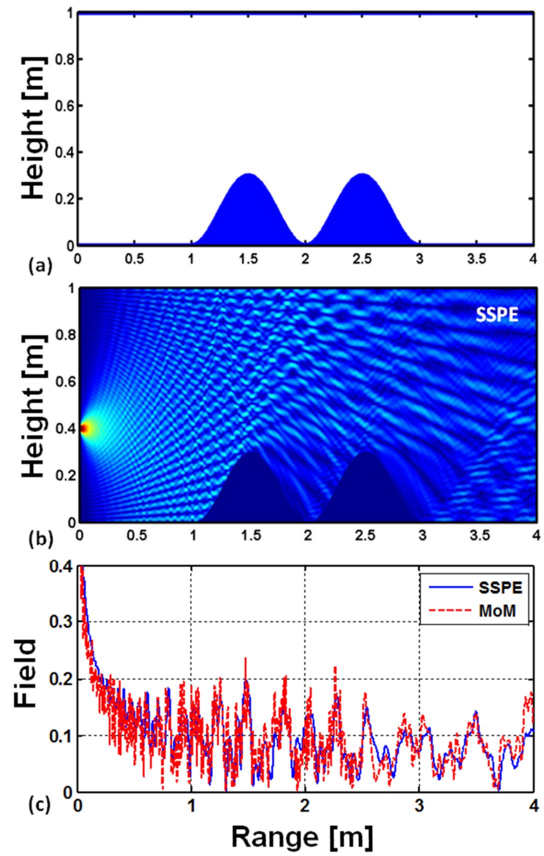

Fig. 10. (a) PEC waveguide with irregular bottom plate, (b) Field map produced with the SSPE, (c) Field vs. z at $x = 0.4$ m, both for TE_z case, (Solid) SSPE, (Dashed) Mi-MoM with 50 iterations ($a = 1$ m, $z' = 0$, $x' = 0.4$ m, $k_0 a = 200$, $\theta_{bw} = 80°$, no tilt, $dz = dx = 0.0025$ m).

VI. CONCLUSIONS

A novel Multi-Iteration Method of Moment (Mi-MoM) procedure is introduced to model the propagation inside resonating structures. A two-dimensional (2D) parallel plate, non-penetrable waveguide is chosen as the test structure.

Mi-MoM results are tested against reference data generated from analytical exact mode summation method and are calibrated. Both the line source excitation and directive antennas are used during these tests. The Mi-MoM approach may increase applicability and efficiency of the MoM which has widely been used in modeling antenna (radiation), propagation, and scattering problems for several decades.

Note that, $\lambda/10$ segmentation is enough for many applications, but up to $\lambda/100$ discretization will be necessary for high-accuracy computations. Finally, direct solution of the MoM matrix system can be achieved up to 8000-10000 segments with a student PC. Beyond this, acceleration techniques are mandatory [5-7].

REFERENCES

[1] R. F. Harrington, *Field Computation by Moment Method*, IEEE Press, New York, 1993.

[2] L. L. Tsai and C. E. Smith, "Moment Methods in Electromagnetics for Undergraduates," *IEEE Trans. Edu.,* vol. E, no. 31, pp. 14-22, 1978.

[3] J. Moore and R. Pizer, *Moment Methods in Electromagnetics: Techniques and Applications*, Research Studies Press, New York, 1984.

[4] M. N. O. Sadiku, *Numerical Techniques in Electromagnetics with MATLAB*, CRC Press, 2009.

[5] H. T. Chou and J. T. Johnson, "Formulation of Forward-backward Method using Novel Spectral Acceleration for the Modeling of Scattering from Impedance Rough Surface," *IEEE Trans. Geo. and Remote Sensing*, vol. 38, pp. 605-607, 2000.

[6] C. A. Tunc, A. Altintas, and V. B. Erturk, "Examination of Existent Propagation Models Over Large Inhomogeneous Terrain Profiles Using Fast Integral Equation Solution," *IEEE Trans. Antennas and Propag.*, vol. 53, pp. 3080-3083, Sep. 2005.

[7] F. Akleman and L. Sevgi, "A Novel MoM- and SSPE-based Groundwave-propagation Field-Strength Prediction Simulator," *IEEE Antennas and Propag. Mag.*, vol. 49, pp. 69-82, 2007.

[8] M. Levy, *Parabolic Equation Methods for Electromagnetic Wave Propagation*, IEE Institution for Electrical Engineers, 1993.

[9] G. Apaydin and L. Sevgi, "Two-way Propagation Modeling in Waveguides with Three-dimensional Finite-element and Split-step Fourier-based PE Approaches," *IEEE Antennas and Wireless Propagation Letters*, vol. 10, pp. 975-978, 2011.

[10] R. Ding, L. Tsang, and H. Braunisch, "Wave Propagation in a Randomly Rough Parallel-plate Waveguide," *IEEE Trans. on MTT*, vol. 57, no. 5, pp. 1216-1223, May. 2009.

[11] L. B. Felsen and A. H. Kamel, "Hybrid Ray-mode Formulation of Parallel Plate Waveguide Green's Functions," *IEEE Trans. Antennas Propag*., vol. 29, no. 4, pp. 637-649, Jul. 1981.

[12] L. B. Felsen, F. Akleman, and L. Sevgi, "Wave Propagation inside a Two-dimensional Perfectly Conducting Parallel Plate Waveguide: Hybrid Ray-mode Techniques and their Visualizations," *IEEE Antennas and Propag. Mag.*, vol. 46, no. 6, pp. 69-89, Dec. 2004.

[13] L. Sevgi, "Guided Waves and Transverse Fields: Transverse to What?," *IEEE Antennas and Propag. Mag.,* vol. 50, no. 6, pp. 221-225, Dec. 2008.

Gökhan Apaydin received the B.S., M.S., and Ph.D. degrees in electrical and electronics engineering from Bogazici University, Istanbul, Turkey, in 2001, 2003, and 2007 respectively. From 2001 to 2005, he was a Teaching and Research Assistant by Bogazici University. From 2005 to 2010, he was a Project and Research Engineer with the Applied Research and Development, University of Technology Zurich, Zurich, Switzerland. Since 2010, he has been with Zirve University, Gaziantep, Turkey. He has been working on several research projects on electromagnetic propagation, the development of a finite-element method for electromagnetic computation, filter design, and related areas. He has (co)authored 19 journals and 30 conference papers.

Levent Sevgi received the Ph.D. degree from Istanbul Technical University, Istanbul, Turkey, and Polytechnic Institute of New York University, Brooklyn, in 1990. Prof. Leo Felsen was his advisor. He was with Istanbul Technical University from 1991 to 1998; TUBITAK-MRC, Information Technologies Research Institute, Gebze/Kocaeli, Turkey, from 1999 to 2000; Weber Research Institute/Polytechnic University of New York, from 1988 to 1990; Scientific Research Group of Raytheon Systems, Canada, from 1998 to 1999; and the Center for Defense Studies, ITUVSAM, from 1993 to 1998 and from 2000 to 2002. Since 2001, he has been with Dogus University, Istanbul. He has been involved with complex electromagnetic (EM) problems and systems for more than 20 years.

Prof. Sevgi is an IEEE Fellow, the Writer/Editor of the "Testing ourselves" Column in the IEEE Antennas and Propagation Magazine and a member of the IEEE AP-S Education Committee.